

# High Pressure, Convectively-Enhanced Laser Chemical Vapor Deposition of Titanium

James Maxwell  
Ramnath Krishnan  
Suresh Haridas

*Institute for Micromanufacturing  
Louisiana Tech University*

*Laser chemical vapor deposition is a freeform technique that can generate three-dimensional structures from organometallic or metal halide precursors. To obtain enhanced growth rates, a novel high pressure reactor has been constructed where impinging jets of volatile fluids are heated and pyrolyzed to create parts. Argon Ion and Nd:YAG lasers have been used to selectively generate three-dimensional titanium shapes from titanium tetrachloride, titanium tetrabromide, and titanium tetraiodide, at pressures up to 3.0 atmospheres. Emission lines characteristic of the reaction rate have been identified which will allow feedback control of the reaction rate. The process is being optimized to obtain high deposition rates, energy efficiency, and desirable material morphologies. A feedback control system is required to generate 3-D structures with dimensional accuracy and predictable deposition rates.*

## I. Introduction

This paper reports the development of a new process which holds promise for the desktop manufacture of metal and ceramic parts at the centimeter scale or larger. Termed high-pressure, convectively-enhanced, laser chemical vapor deposition (HPCE-LCVD), the process employs convective flows of precursor gases to enhance the growth rate of vapor-phase solid freeform fabrication (SFF). Preliminary results in the growth of titanium from the titanium halides at moderate pressures and flowrates (up to 3 atmospheres) are presented herein. These early results will be used to evaluate the utility of each precursor for future use in the HPCE-LCVD apparatus.

### A) Three-Dimensional LCVD

Derived from chemical vapor deposition (CVD), *pyrolytic* laser chemical vapor deposition (LCVD) employs a scanning laser beam to selectively *heat* portions of a substrate, and in this way induce a localized CVD reaction.<sup>1</sup> If the growth is not self-limiting either due to the deposit material being highly-conductive,<sup>2</sup> being highly-reflective of the laser light,<sup>3,4</sup> or having a low melting point,<sup>5</sup> then high-aspect ratio microstructures may be grown, such as those shown in Fig. 5. Careful adjustment of the laser power may be required during the transient growth<sup>6</sup> of metals to obtain continuous, uniform dimensions--as will be seen in this paper, where the growth of titanium is thermally-self-limiting at low pressures (see Fig. 3).

Several authors have explored the possibilities of three-dimensional growth using LCVD, prototyping rods,<sup>7</sup> fibers,<sup>8</sup> coils,<sup>9</sup> blocks,<sup>10</sup> and more complex structures.<sup>11</sup> Rods have been grown of aluminum,<sup>12</sup> alumina,<sup>13</sup> gold,<sup>14</sup> nickel,<sup>15</sup> tungsten,<sup>16</sup> silicon,<sup>17</sup> chromium-oxide,<sup>18</sup> iron,<sup>19</sup> steel,<sup>20</sup> and boron.<sup>21</sup> It is noteworthy, however, that the materials with the greatest thermal conductivities, e.g. aluminum, gold, and tungsten, are highly irregular in shape, whilst

continuous, steady-state rod growth was readily demonstrated with the other materials. Materials with high thermal conductivity also tend to grow more broadly, or in the extreme case, only as hemispheres.<sup>22</sup> Thus, controlled growth of highly-conductive metals is a needed goal.

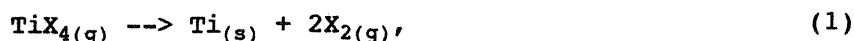
One method for increasing the aspect ratio of a metal deposit is to use a pulsed-laser or a chopped beam.<sup>23</sup> This method was employed throughout the Ti growth experiments. Another method for obtaining controlled freeform growth was previously demonstrated by the author;<sup>24</sup> where spectral emissions generated during an LCVD reaction were measured to determine the volumetric growth rate. This measure was then used to automatically compensate for errors in the growth, adjusting the incident laser power and other process inputs in real-time. This technique will be required for controlled growth of titanium, whose bulk thermal conductivity is 21.9 W/m-K at 300K.

### **B) Mass Transport Effects and the Growth Rate**

While low-pressure LCVD processes are much too slow for macro-scale prototyping, the volumetric deposition rate rises with pressure. At pressures above 1 atmosphere, Wallenberger *et al.* recently reported volumetric growth rates of nearly 0.1 mm<sup>3</sup>/s.<sup>25</sup> This rate increase occurs from greater adsorption of the precursor onto the reaction surface, as well as from enhanced natural convection--which permits more rapid transport to (and from) the surface. The growth rate continues to rise with pressure until the fluid reaches a critical pressure;<sup>26</sup> for the metal halides, this critical pressure typically lies in the range of 25-100 atmospheres. Thus, by directing a forced flow of precursor fluids onto a heated reaction zone, an enhanced deposition rate is obtained, allowing parts to be grown quickly. This is the principle behind the HPCE-LCVD process. An added benefit is that the use of high pressures favors the growth of amorphous or fine-grained polycrystalline materials--which possess greater strength than cast, extruded, or sintered materials. These effects will be demonstrated later in this paper, where fine-grained, titanium rods were grown at enhanced rates.

### **C) Chemical Vapor Deposition of Titanium**

The titanium halides are commonly employed for the chemical vapor deposition of titanium. These are pyrolyzed either directly, or by hydrogen reduction at temperatures above 1500 K.<sup>27</sup> The overall reactions are:



where X=Cl, Br, or I, respectively. Titanium thin films have been deposited from TiCl<sub>4</sub>,<sup>28,29</sup> as well as from TiBr<sub>4</sub>.<sup>30</sup> TiO<sub>2</sub> films have also been deposited<sup>31</sup> from a mixture of TiCl<sub>4</sub>, H<sub>2</sub>, and CO<sub>2</sub>--while titanium dioxide rods have been grown from TiCl<sub>4</sub>, H<sub>2</sub>, and atmospheric oxygen.<sup>32</sup>

## **II. Experimental**

### **A) Moderate Pressure Experiments (to 1.5 bar)**

The titanium growth experiments were carried out in a heated stainless steel reactor as shown in Fig. 1. The reactor (A) consisted of a six-way cross, with windows on two sides, one for laser input (B) and another for cross-illumination of the sample (not shown). A UV-grade fused-silica window was located for observation at right angles to the laser input and opposite the illumination source. A microscope and CCD camera were used to monitor the growth.

Throughout the experiment, a 90 mm focal-length, gradient-index lens (C) was used to focus the gaussian input beam to a 1/e<sup>2</sup> spot size of approximately 50 microns. A Coherent Innova 70 argon-ion laser with output power to 2.2 W TEM<sub>00</sub> (8 Watts Multimode) was used at

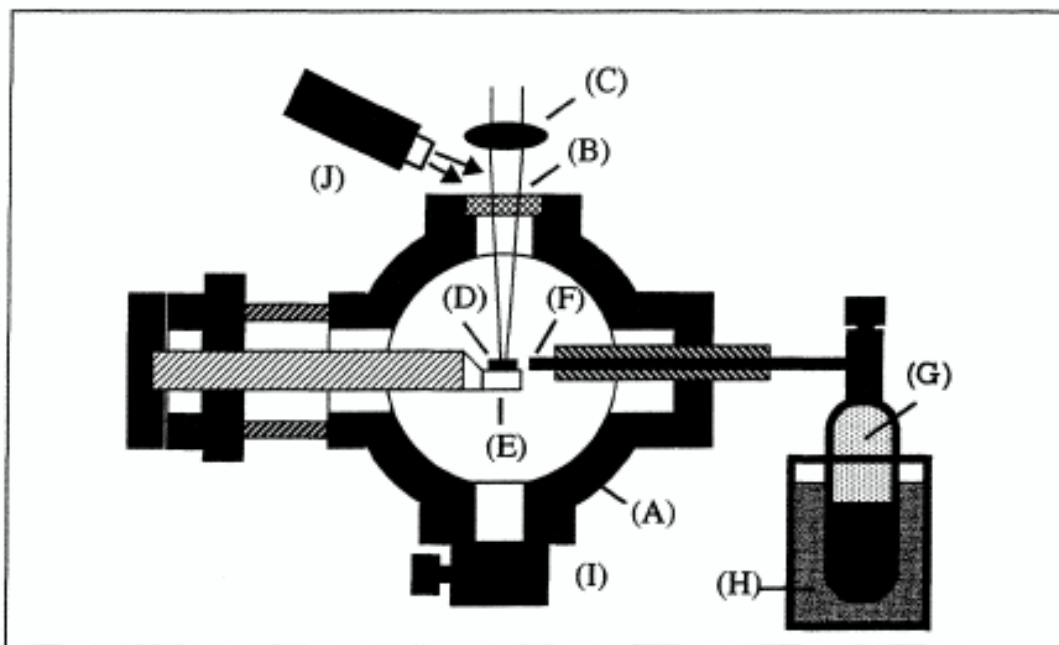


**Fig. 1: Apparatus for Moderate Pressure Experiments**

the primary 488/514 nm lines; this laser was readily interchanged with a Lee Laser 40 W (10 W TEM<sub>00</sub>) Nd:YAG laser. This was operated in cw mode at 1064 nm.

A variety of substrates (D) were employed to initiate sample growth. Experiments were performed using bare titanium, glassy carbon, and graphite disks. The latter two were chosen for their low spectral reflectances and high melting points. All substrates were mounted on a sample holder (E), attached to a micromanipulator, allowing the substrate to be scanned relative to the beam focus.

Reactants were introduced into the reactor via a 1/16" stainless steel entrance tube (F), which could be independently heated at the nozzle exit to temperatures up to 2400 K. Since titanium tetrachloride is a liquid at room temperature with a boiling point of 137 C, and titanium tetrabromide and tetraiodide boil at 230 C and 377 C respectively, each precursor was first heated in a sample cylinder (G) to obtain a sufficient vapor pressure for growth. The sample cylinders were heated in a beaker of water or ethylene glycol (H). During the static growth experiments, the precursor vapor pressure was prescribed by the temperature of this heated sample cylinder (G), while for the convective experiments, the roughing valve (I) was opened, allowing the overall chamber pressure to drop to less than 50 mbar; in this way, a constant flow was obtained down the 1/16" stainless steel entrance tube (F), which could be preheated and directed toward the sample (D). The entire assembly was wrapped with heater tape and insulation, except for the windows, to maintain a constant chamber temperature above that of the sample cylinder. To eliminate condensation of the precursor on the laser window, a hot air gun (J) was directed at the window, at a temperature equal to or greater than that of the chamber.

### **B) Design of the High-Pressure Experimental Apparatus (to 300 bar)**

In parallel with the apparatus described above, a high-pressure vessel has been constructed which will allow further investigation of metal deposition at much greater growth rates. The high-pressure chamber has been designed for operation up to 300 atmospheres, and has three fused-silica, Poulter-sealed windows, as shown in Fig. 2, allowing up to three orthogonal laser beams to be focused simultaneously to a common point (A). The high pressure reactor (B) is enclosed inside a heavy steel dome (C), which acts both as furnace and fume hood. Two

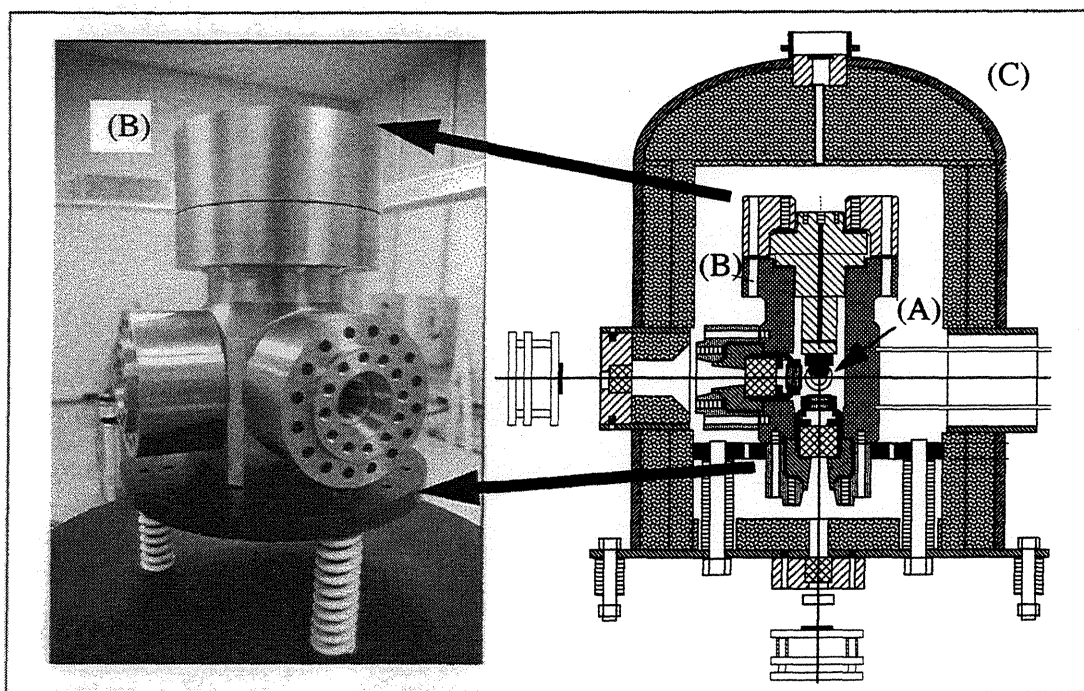


**Fig. 2: High Pressure Assembly and Reactor**

3000 W heaters circulate hot air around the reactor, allowing the windows to be warmed to the same temperature as the chamber. Laminated graphite and stainless steel gaskets are being employed to seal the windows and reactor cap, allowing chamber temperatures of up to 500 C. Precursor gases are supplied from a high-pressure evaporator (not shown), and are directed toward the laser focus (A) through a small nozzle. The chamber is evacuated using a simple Venturi pump, and reaction by-products are passed through a burn box to the clean room scrubber.

To scan the laser focus inside the chamber, four high-pressure motion feedthroughs are being installed in the lower portion of the reactor; these are attached to internal stages which position the sample and allow for three linear and one rotational degree of freedom. In addition, two orthogonal beams will be modulated at the common focus, providing one more degree of freedom (tilt). In this way, completely arbitrary structures may be fabricated.

### III. Results

Experiments with the titanium halides at *low pressures* were unimpressive. At the room-temperature vapor pressure of  $\text{TiCl}_4$  (i.e. at abt. 13 mbar), no growth was observed on the glassy carbon substrates up to their softening temperature (abt. 1500 K). At higher pressures, the *transient* growth rate of each precursor improved steadily on the graphite and titanium substrates. Samples (A), (B), and (C) in Fig. 3, were successfully grown at  $\text{TiCl}_4$ ,  $\text{TiBr}_4$  and  $\text{TiI}_4$  vapor pressures of 330, 8.5, and 180 mbar, respectively, and at transient rates of up to  $0.37 \mu\text{m/s}$ . Titanium tetrachloride, with its greater vapor pressure, exhibited the highest growth rates, but only at temperatures approaching the melting point of Ti (1953 K). To initiate growth with this precursor, we first ablated a portion of the titanium substrate, then lowered the average power (or defocused the beam) until the substrate could no longer be melted (10 W,  $60 \mu\text{m}$  spot size). Growth could then be initiated at incident powers as low as 4.3 W. Using the well-known expression for the peak temperature rise of a Gaussian beam on a semi-infinite solid (1):

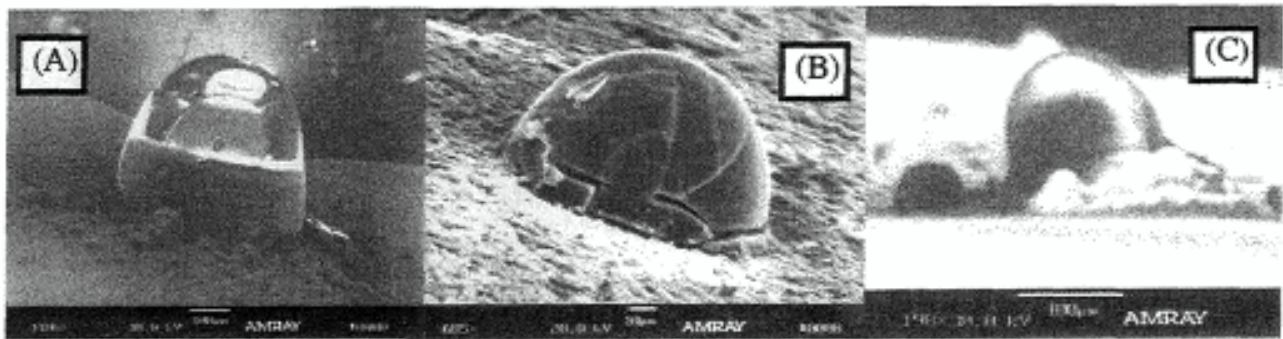


**Fig. 3: Titanium Shapes from the Ti Halides**

$$T_p = \frac{P(1-R)}{\sqrt{\pi\kappa\omega_o}}, \quad (1)$$

this initial power indicates a  $\text{TiCl}_4$  threshold deposition temperature of approximately 1130 K. Below this temperature no thick Ti films or rods were formed.

At similar incident powers, titanium iodide yielded growth rates nearly commensurate with that of  $\text{TiCl}_4$ , although at a fraction of the vapor pressure. It also exhibited a lower threshold deposition temperature of abt. 870 K (3 W incident power), which is consistent with reports that it possesses an activation energy lower than that of  $\text{TiCl}_4$ .<sup>33</sup> The growth rate from  $\text{TiBr}_4$  was less impressive, giving rates of at most  $0.04 \mu\text{m/s}$ , at pressures up to 8.5 mbar. Thermodynamic calculations, minimizing the Gibb's free energy, confirmed that little deposition is likely to occur from pure  $\text{TiBr}_4$  at temperatures up to the melting point of titanium.<sup>34</sup> However, further experimentation at higher vapor pressures will be necessary to determine the potential of this precursor for HPCE-LCVD.

Overall, titanium growth tended to be thermally self-limiting. This is illustrated in Fig. 4, where rods were grown for 30 minutes each from  $\text{TiI}_4$  at a variety of vapor pressures. Note that

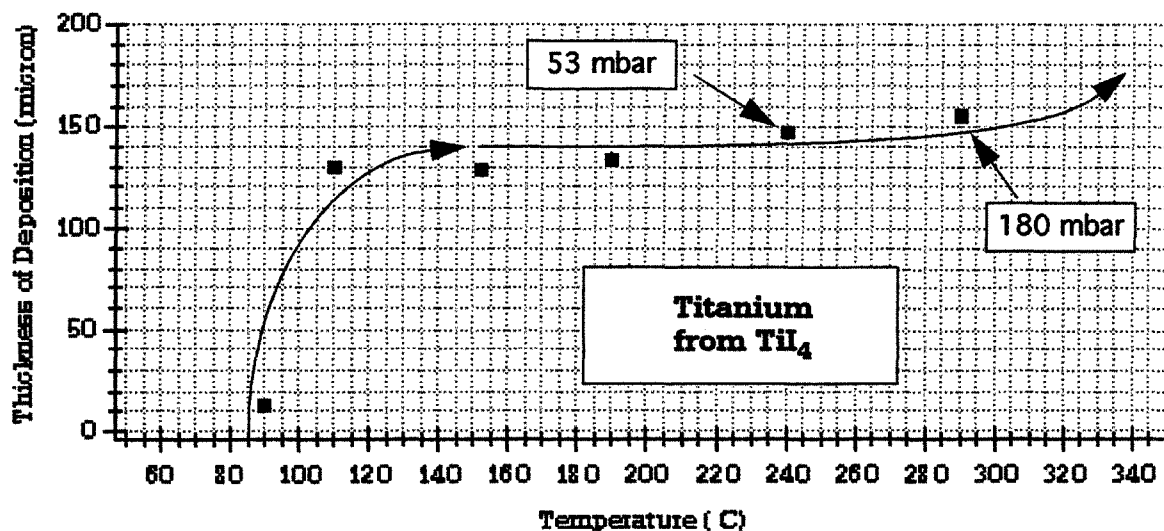


**Fig. 4: Low-Pressure Transient Titanium Growth vs. Evaporator Temp.**



after initial rapid transient growth, each rod approaches a limiting height. This can be explained either by rapid cooling as the deposit grows (and losses increase to its surroundings), or by overheating and melting as the rod grows away from the substrate (which acts diminishingly as a heat sink). To explore this self-limiting effect, the laser power was ramped up slowly, from an initial power of 6 W to over 10 W; surprisingly, this did not yield tall deposits as well as the opposite approach, i.e. lowering the power from an initially high temperature. Thus, since insufficient convection occurs, the temperature increases<sup>6</sup> as the rod lengthens, and the rod subsequently overheats and melts. Evidence of melting can also be seen in Fig. 3 (A), where the self-limiting rod height was attained. Clearly, steady-state<sup>6</sup> rod growth cannot be obtained at low gas pressures unless the temperature of the deposit is lowered continuously in a controlled manner--and with the titanium halides little latitude exists between the temperature at which growth initiates and the melting point of Ti--making the reaction especially difficult to control.

At *higher* vapor pressures, however, gas convection begins to contribute significantly to the heat losses, giving rise to a steady-state temperature distribution at the rod tip--and allowing continuous 3-dimensional growth without temperature control. For titanium tetrachloride, this was realized at pressures above 2000 mbar, as can be seen in Fig. 5. At 3000 mbar, Ti rods over 1 mm long were grown without changing the laser focus or the average power. By gradually increasing the laser power as the rod grew (to compensate for the stationary laser focus and diminishing beam intensity), rods up to 4 mm long could be grown at axial rates up to 1.4  $\mu\text{m/s}$ . In addition, rods grown at the highest pressures exhibited no apparent grain structure, down to 100 nm or less. This confirms the results of Wallenberger,<sup>25</sup> who also obtained fine-grained

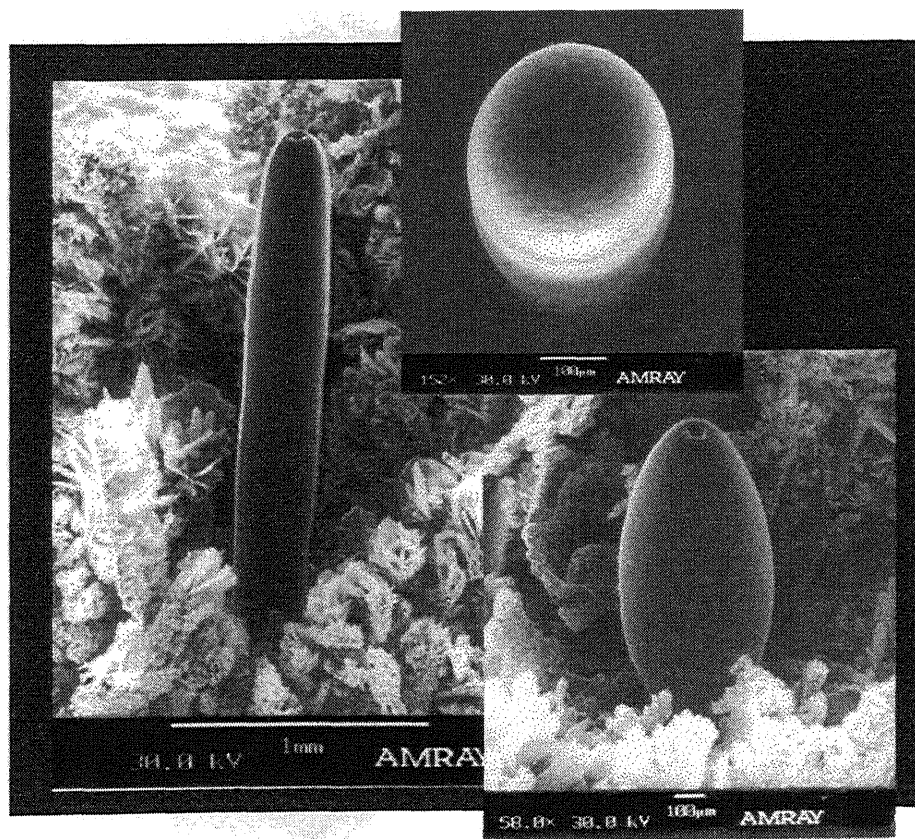


**Fig. 5: Titanium Rods Grown at High Pressure**

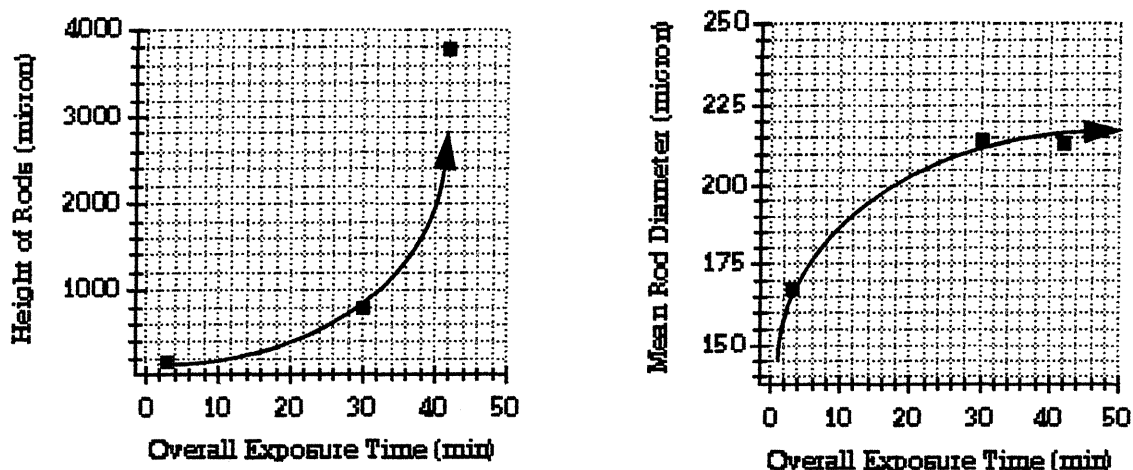


**Fig. 6: Rod Height and Diameter vs. Laser Power**

and amorphous rods at high vapor pressures. In Fig. 6, the height and diameter of the Ti rods are also plotted vs. exposure time. As expected for steady-state growth, the rod height increases without bound, and the rod diameter approaches a constant (steady-state) radius.

During the high-pressure reaction, a broad band of blue-violet emission lines were also observed, well below the blackbody emissions--which appeared to peak in the yellow portion of the spectrum. These have been identified as the strong 455-468 nm emission lines of the singly ionized  $\text{Cl}_2^+$  molecule, a by-product of the  $\text{TiCl}_4$  reaction.

Analysis of the Ti rod composition was carried out with an X-ray diffractometer. Combined results from several samples indicated that the rods were primarily pure Ti, with small quantities of  $\text{TiO}_2$ . No  $\text{TiCl}_3$  was found to be present in the rods, although this solid by-product formed readily in a ring around the Ti rods. The titanium rods were exposed to atmospheric oxygen prior to the X-ray analysis. Further measurements will be conducted using a scanning Auger microprobe to determine the extent of oxide contamination within the rods.

#### **IV. Conclusions**

To obtain continuous Ti growth, sufficient precursor pressure must be present for natural convection to establish a constant temperature distribution over the reaction zone. Without this convective heat loss, it is difficult to sustain growth; the temperature must be monitored continuously to avoid melting the deposit. In addition, gas convection enhances transport of the precursor to the reaction, raising the volumetric growth rate by more than an order of magnitude.

While steady-state growth may be obtained using  $\text{TiCl}_4$  at high pressures, the greatest promise for HPCE-LCVD may be  $\text{TiI}_4$ , which exhibits the largest latitude between its threshold temperature and the melting point of titanium, facilitating growth control. Further work will study the deposit composition and growth rates of these precursors at significantly higher pressures--up to their critical points. In addition, the emission spectra discovered at 455-468 nm will be used to control the growth of the  $\text{TiCl}_4$  reaction using the emissions feedback technique.

#### **V. Acknowledgments**

Our appreciation goes to the Louisiana Education Quality Support Fund (LEQSF) and the College of Engineering and Science at Louisiana Tech for their support of this work.

## VI. Bibliography

1. Bäuerle, D., Springer Series in Chemical Physics 39, (1984), pp. 166-182.
2. Allen, S. D., Jan, R. Y., Edwards, R. H., Mazuk, S. M., Vernon, S. D., Proc. of SPIE, Laser Assisted Deposition, Etching, and Doping, Vol 459, (1984), pp. 42-48.
3. Meunier, M., Izquierdo, R., Desjardins, Thin Solid Films, Vol. 218, (1992), pp. 137-143.
4. Allen, S. D., Jan, R. Y., Mazuk, S. M., Vernon, S. D., J. Appl. Phys., Vol. 58, No. 1, (1 Jul. 1985), pp. 327-331. [344]
5. Westberg, H., Boman, M., Norekrans, A.-S., Carlsson, J.-O., Thin Solid Films, Vol. 215, (1992), pp. 126-133.
6. Maxwell, J. L., Ph.D. Thesis, Rensselaer Polytechnic Institute, (1996).
7. Bäuerle, D., Leyendecker, G., Wagner, D., Applied Physics A, Vol. 30, (1983), pp. 147-149.
8. Leyendecker, G., Bäuerle, D., J. Electrochem. Soc., Vol. 130, No. 1, (1983), pp. 157-160.
9. Westberg, H., Boman, M., IEEE MEMS Conference Proc., (Feb. 1992), p. 172.
10. Zong, G.-S., Ph.D. Thesis, University of Texas at Austin, (1992).
11. Wanke, M.C., Lehmann, O., Muller, K., Wen, Q, Stuke, M., Science, Vol. 275, (28 Feb. 1997), pp.1284-1286.
12. Rytz-Froidevaux, Y., Salathé, R. P., Gilgen, H. H., Physics Letters, Vol. 84A, No. 4, (27 Jul. 1981), pp. 216-218.
13. Lehmann, O., Stuke, M., Materials Letters, Vol. 21, (Oct. 1994), pp. 131-136.
14. Comita, P. B., Kudas, T. T., J. Appl. Phys., Vol. 62, No. 6, (15 Sep. 1987), pp. 2280-2285.
15. Kräuter, W., Bäuerle, D., Fimberger, F., Appl. Phys. A, Vol. 31, (1983), pp. 13-18.
16. Allen, S. D., Tringubo, A. B., J. Appl. Phys., Vol. 54, No. 3, (Mar. 1983), pp. 1641-1643.
17. Westberg, H., Boman, M., Johansson, S., Schweitz, J.-A., J. Appl. Phys., Vol. 73, No. 11, (1 Jun. 1993), pp. 7864-7871.
18. Arnone, C., Rothschild, M., Black, J. G., Ehrlich, D. J., Appl. Phys. Lett., Vol. 48, No. 15, (14 Apr. 1986), pp. 1018-1020.
19. Maxwell, J., Pegna, J., DeAngelis, D., Messia, D., Material Research Society Symposium Proceedings, v. 397 (B3.30): Fall 1995 Meeting, Boston, MA (Nov. 27--Dec.1, 1995).
20. Ibid.
21. Wallenberger, F. T., Nordine, P. C., Materials Letters, Vol. 14, No. 4, (1992), pp. 198-202.
22. Baum, T. H., Larson, C. E., High Temperature Science, Vol. 27, (1990), pp. 237-249.
23. Morishige, Y., Kishida, S., Appl. Phys. A, Vol. 59, (1994), pp. 395-399.
24. Maxwell, J., Pegna, J., DeAngelis, D., (Accepted for Publ.: Applied Physics A, Aug. 1996)
25. F.T. Wallenberger, P.C. Nordine, Science, 260, 66-68 (1993)
26. Bradley, R. S., High Pressure Chemistry, Pergamon Press, Oxford, NY (1965), p. 101.
27. Pierson, H. O., Handbook of Chemical Vapor Deposition, Noyes Publications, Westwood, NJ, (1992), pp. 146-148.
28. Izquierdo, R., Lavoie, C, Meunier, M., MRS Symposium, Vol. 158, (1993), pp. 141-146.
29. Alexandrescu, R., Cireasa, R., Dragnea, B., Morjan, I., Voicu, I., Andrei, A., Vasiliu, F., Popescu, C., Advanced Materials for Optics and Electronics, Vol. 5, (1995), pp. 19-30.
30. Chou, W. B., Azer, M. N., Mazumder, J., J. Appl. Phys., Vol. 66, No. 1, (1989), pp. 191-195.
31. Allen, S. D., J. Appl. Phys., Vol. 52, No. 11, (Nov. 1981), pp. 6501-6505.
32. Jakubenas, K., Marcus, H.L., Solid Freeform Fabrication Symposium, (1995), pp. 381-388.
33. Eizenberg, M., Materials Research Society Bulletin, Vol. 20, No. 11, (Nov. 1995), p.38.
34. Boman, M., Personal Communication, Univ. of Uppsala, Sweden (1997).